HHS Public Access

Author manuscript

Drug Discov Today Technol. Author manuscript; available in PMC 2018 April 14.

Published in final edited form as:

Drug Discov Today Technol. 2017 March ; 23: 27–36. doi:10.1016/j.ddtec.2017.03.002.

The Production of 3D Tumor Spheroids for Cancer Drug Discovery

Shilpa Sant[1,2,3] and **Paul A. Johnston**[1,4,$]

[1]Department of Pharmaceutical Sciences, School of Pharmacy, Pittsburgh, Pennsylvania 15261

[2]Department of Bioengineering, Swanson School of Engineering, Pittsburgh, Pennsylvania 15261

[3]McGowan Institute for Regenerative Medicine, Pittsburgh, Pennsylvania 15261

[4]University of Pittsburgh Cancer Institute, University of Pittsburgh, Pittsburgh, Pennsylvania 15261

Abstract

New cancer drug approval rates are ≤ 5% despite significant investments in cancer research, drug discovery and development. One strategy to improve the rate of success of new cancer drugs transitioning into the clinic would be to more closely align the cellular models used in the early lead discovery with pre-clinical animal models and patient tumors. For solid tumors, this would mandate the development and implementation of three dimensional (3D) *in vitro* tumor models that more accurately recapitulate human solid tumor architecture and biology. Recent advances in tissue engineering and regenerative medicine have provided new techniques for 3D spheroid generation and a variety of *in vitro* 3D cancer models are being explored for cancer drug discovery. Although homogeneous assay methods and high content imaging approaches to assess tumor spheroid morphology, growth and viability have been developed, the implementation of 3D models in HTS remains challenging due to reasons that we discuss in this review. Perhaps the biggest obstacle to achieve acceptable HTS assay performance metrics occurs in 3D tumor models that produce spheroids with highly variable morphologies and/or sizes. We highlight two methods that produce uniform size-controlled 3D multicellular tumor spheroids that are compatible with cancer drug research and HTS; tumor spheroids formed in ultra-low attachment microplates, or in polyethylene glycol dimethacrylate hydrogel microwell arrays.

Introduction

New cancer drug leads are typically identified in high throughput growth inhibition screening (HTS) campaigns prosecuted in panels of tumor cell lines that are maintained and

[$]Corresponding Author: Paul A. Johnston Ph.D., Research Associate Professor, Department of Pharmaceutical Sciences, School of Pharmacy, Room 548 Salk Hall, 3501 Terrace Street, Pittsburgh PA 15261. paj18@pitt.edu.

Conflict of interest

The author(s) have no conflict of interest to declare.

assayed in two dimensional (2D) cell culture models executed in serum containing medium [1–3]. Cytotoxic compounds are progressed to anti-tumor efficacy studies in mice, and mechanism of action studies (MOAs) are initiated for compounds that demonstrate *in vivo* efficacy [2, 4, 5]. For molecularly targeted agents developed to counteract the specific oncogenic alterations of tumor cells, biochemical or cell based screens typically precede these steps [1–3]. However, despite significant investments in cancer research, drug discovery and development, new cancer drug approval rates are ≤ 5%, significantly lower than for other therapeutic areas, and most advanced stage metastatic tumors remain incurable [2, 4, 5]. Several factors have contributed to the poor success of anticancer drug development: preclinical models fail to adequately recapitulate the complexity and heterogeneity of human cancers; there is often a reliance on multi-component ill-defined proliferation or angiogenesis endpoints rather than discrete molecular targets and pathways; and occasionally drug candidates with suboptimal pharmacological properties and/or insufficient translational research have been inappropriately advanced to the clinic [2, 4, 5]. Although preclinical animal studies rely heavily on mouse tumor models such as murine tumors transplanted into syngeneic mice, genetically engineered mouse models, or xenograft models, cancer models in mice have some significant limitations; murine tumors do not behave like human tumors, the stromal components are not of human origin, tumor implantation sites are often not the natural tumor location, the immune system is compromised in xenograft models, and xenograft tumor growth rates are typically faster than primary human tumors [2, 4, 5]. Patient derived xenograft (PDX) models that have never been adapted to tissue culture have been implemented to improve the correlation between preclinical animal models and clinical trial drug responses [6–8]. Another strategy that could significantly improve the rate of success of new cancer drugs transitioning into the clinic would be to more closely align the cellular models used in the early lead discovery with pre-clinical animal models and patient tumors [2, 9–12]. For solid tumors, this would mandate the development and implementation of three dimensional (3D) *in vitro* tumor models that more accurately recapitulate human solid tumor architecture and biology [9–12].

Solid tumors are composed of tumor and stromal cells (vascular, immune and fibroblast cells) and extracellular matrix (ECM) components existing in a highly interactive 3D microenvironment where cell-cell interactions, cell-ECM interactions and local gradients of nutrients, growth factors, secreted factors and oxygen regulate cell function and behavior (Fig. 1) [13–17]. Compared to 2D monolayer cultures, tumor cells cultured in 3D microenvironments experience different cellular cues that modify their responses to various stimuli [13–25]. For example, tumor cells growing in 3D cell cultures are exposed to dramatically different adhesive, topographical and mechanical forces than cells growing in 2D on treated surfaces [13, 14, 17, 18, 20, 21]. Additionally, the cell-cell and cell-ECM interactions of cells in solid tumors and multi-layer tumor spheroids constitute a permeability barrier through which therapeutic agents must penetrate [13–25]. It has been well documented that the 3D microenvironment alters numerous cellular and functional activities including; morphology, signal transduction, histone acetylation, gene expression, protein expression, drug metabolism, differential zones of proliferation, viability, hypoxia, pH, differentiation (epithelial to mesenchymal transition, EMT), migration, and drug sensitivity [13–25]. When cancer drug responses have been directly compared in 2D and 3D

tumor cell culture models, differential drug sensitivity between the two models can be manifested as either greater resistance or enhanced sensitivity [13, 14, 17, 18, 20, 21]. In consequence, a broad consensus has emerged that *in vitro* 3D tumor cell cultures provide more appropriate preclinical models to evaluate the potencies of cancer drug leads for solid tumors, and that the application of these models have the potential to improve the success rate of drug candidates that advance into mouse tumor models and clinical trials. It should be noted however that the application of 3D cell culture models to cancer drug discovery is not a new concept, indeed for almost 50 years, soft agar colony formation assays have been the gold standard *in vitro* method used to establish the transformation status of cells and for testing new drug candidates in low throughput [12, 22, 26–30].

Soft agar colony formation assays (SACF)

The ability of cells to grow in an anchorage-independent manner in semisolid medium is the defining characteristic of malignantly transformed cells [12, 22, 26–30]. SACF assays measure the clonogenicity of tumor stem cells which represent < 0.4% of the total cells in a solid tumor but are able to divide and form anchorage-independent 3D colonies in semisolid agar [12, 27]. In contrast, differentiated tumor cells and stromal cells do not grow or form 3D colonies in semisolid medium. Human tumor cell lines, cells freshly isolated from patient tumors, and cells isolated from PDX's serially passaged in nude mice are all compatible with SACF assays [12, 27]. Hematopoietic stem cells isolated from bone marrow, peripheral blood or umbilical cord blood also form anchorage-independent 3D colonies in semisolid agar and are often used as normal cell controls to evaluate whether a new cancer agent is tumor specific or might have a workable therapeutic index [12,27]. SACF assays have typically been implemented to validate lead compounds identified in 2D tumor cell line HTS growth inhibition assays before they progress in the cancer drug discovery pipeline [12, 22, 27]. However, SACF assays have some drawbacks that restrict their throughput and widespread application to cancer drug discovery (Table 1): the protracted 2–3 week duration of assays is both rate-limiting and resource intensive; assays are usually performed in petri dishes or 6-well, 12-well or 24-well microtiter plates thereby severely limiting throughput and capacity; the agar must be heated and mixed with tumor cells without compromising viability; configuring 3-layer SACF assays is a complex multi-step procedure challenging to automate and the temperature of the agar must be strictly controlled to prevent premature gelation during automated liquid transfers; quantifying the number of colonies growing in semisolid medium is difficult; and SCAF assays are both labor intensive and require experimentalists with extensive expertise and experience to implement them properly [12, 22, 26–30]. In addition, not all transformed tumor cells perform well in SACF assays. For instance, many head and neck cancer (HNC) cell lines that readily form xenograft tumors in immune deficient mice do not form colonies in soft agar [31]. Despite these challenges, automated 96-well [28] and 384-well [22, 30] SACF assays have recently been developed and implemented for cancer drug screening. However, to date HTS SACF assays have only been used to screen small scale collections of 1,528 natural products or 9,600 compounds in a 10-drug mixture format, and only against single tumor cell lines [22, 30]. Since the genetic diversity and heterogeneity of cancer dictates that multiple cell models and signaling pathways should be interrogated, additional 3D tumor models compatible with HTS have been sought as a strategy to improve the correlation

between early preclinical *in vitro* assays and efficacy in preclinical mouse tumor models and ultimately against patient tumors.

3D tumor spheroids

3D tumor spheroids are self-assembled cultures of tumor cells formed in conditions where cell-cell interactions predominate over cell-substrate interactions [14, 16–18, 32, 33]. Multicellular tumor spheroids resemble avascular tumor nodules, micro-metastases, or the intervascular regions of large solid tumors with respect to their morphological features, microenvironment, volume growth kinetics and gradients of nutrient distribution, oxygen concentration, cell proliferation and drug access (Fig. 1) [14, 16–18, 32, 33]. Recent advances in tissue engineering and regeneration have provided new techniques for 3D spheroid generation and a variety of anchorage-dependent and anchorage-independent i*n vitro* 3D cancer models have been explored; tissue slices or explants, gel or matrix embedded cultures and co-cultures, scaffold-based supports, micro-patterning and cell printing approaches, microfluidic systems, and multicellular spheroids (Table 1) [14–19, 21, 23–25, 32–42]. Although 3D models incorporating the stromal cell populations that make significant contributions to the tumor microenvironment would be more physiologically relevant, the added complexity presents some significant technical challenges for HTS and drug discovery. This review focuses mainly on 3D models comprised of only tumor cells.

Anchorage-dependent tumor spheroids

Anchorage-dependent models utilize engineered scaffolds designed to simulate the ECM and provide structural or physical support. Hydrogels containing proteins and ECM components are used to encapsulate cancer cells in micro-porous scaffolds that mimic native ECM and enable cells to adhere, proliferate, spread and migrate in 3D [13, 15, 19, 20, 22, 23, 34, 36, 37]. However, natural gel matrices such as the widely used matrigel contain an ill-defined myriad of growth factors and endogenous components that may exhibit considerable batch to batch variability, and temperature shifts required for gelation can be challenging to automate. Reproducible calibration of the mechanical and biochemical properties of naturally derived hydrogels can also be difficult. Some of these limitations may be overcome by the use of covalently modified synthetic hydrogels, often based on poly ethylene glycol (PEG) [36]. However, the variable Z-plane locations of 3D colonies, heterogeneity in the size and shape of 3D colonies, and the opacity of gels or matrices can present a challenge to HTS signal capture and/or analysis. Hydrogels may also limit the penetration of compounds and detection reagents, and for some assay formats, the gels must be dispersed and the cells isolated for subsequent analysis, thereby losing the ability to capture any spatial information. Despite such limitations (Table 1), several groups have developed 3D tumor models in hydrogel scaffolds and used these cultures to assess the potency of small numbers of cancer drugs or for small pilot screens of ≤1,500 compounds [20, 22, 23, 34, 36].

Anchorage-independent tumor spheroids

Several methods to generate anchorage-independent 3D tumor spheroids have also been developed; spontaneous aggregation, liquid overlay on agarose, hanging drop cultures, spinner flask cultures, rotary cell culture systems, ultra-low attachment (ULA) plates, and

encapsulation in biologically inert hydrogels lacking attachment cues (Table 1) [14, 16–18, 21, 24, 25, 32, 33, 38, 39]. However, not all tumor cell lines form 3D spheroids under these conditions [14, 33], and many of these methods generate irregular 3D cellular aggregates that have a wide range of morphologies and sizes [16, 17]. Additionally, some of these anchorage-independent 3D tumor spheroid methods are labor intensive and involve protracted tissue culture periods, and to date, these cultures have only been implemented for pilot screens of ≤1,200 compounds [18, 21, 24, 33].

Implementation of 3D tumor models for HTS

Despite the availability of homogeneous assay methods and high content imaging approaches to assess tumor spheroid morphology, growth and viability [38], some of the technical challenges described above have restricted the implementation of 3D models in HTS (Table 1) [18, 20–22, 24, 33, 34]. Perhaps the most significant obstacle to achieve acceptable HTS assay performance metrics occurs in 3D tumor models that produce spheroids with large variations in morphologies and size. Below we highlight two methods that produce uniform size-controlled 3D multicellular tumor spheroids that are amenable to cancer drug research and HTS.

Ultra-low attachment microplates

In 2012, Vinci *et al* published methods to establish and analyze 3D tumor spheroids generated in 96-well U-bottomed ultra-low attachment microplates (ULA-plates) [33]. U-bottomed 96-well ULA-plates treated with a hydrophilic, neutrally charged coating covalently bound to the polystyrene well surface supported the growth and formation of tight spheroids, compact aggregates, or loose aggregates in a variety of human tumor cells lines [33]. Tumor spheroids formed in 96-well U-bottomed ULA-plates exhibited similar morphologies and immuno-histochemistry staining to spheroids grown in agar, and could be used for tumor cell migration and invasion assays [33]. Ekert *et al* demonstrated that eight lung cancer cell lines underwent self-assembly to form viable 3D tumor spheroids in 96-well ULA-plates, and when compared to 2D cultures, 3D cultures exhibited altered Epidermal growth factor receptor (EGFR) and cMET expression levels and signaling [18]. The ULA spheroid culture environment changed the lung tumor cellular responses to drugs and growth factors and mimicked the natural tumor microenvironment better than corresponding 2D cultures [18]. Non-transformed breast epithelial cells and breast cancer epithelial cells were cultured as 3D spheroids in 96-well ULA-plates either alone or as co-cultures with human fibroblasts or HUVECs [43]. When compared to 2D cultures, microtubule disrupting agents and EGFR inhibitors exhibited preferential cytotoxicity against breast cancer cells over normal cells when cultured as 3D spheroids [43]. Selective breast cancer drug sensitivity was also observed in 3D co-cultures when compared to 2D co-cultures [43]. Consistent with the SACF assays discussed above, Rotem and colleagues have reported that transformed cell lines grow in low attachment plates but that non-transformed cells do not [44]. H-RAS-transformed fibroblasts were screened against 633 compounds from the NIH clinical collection and a small kinase focused library in growth inhibition assays conducted in 2D monolayers or in 3D cultures grown in ULA-plates [44]. Four drugs inhibited H-RAS fibroblast growth in 3D exclusively, and five preferentially inhibited growth in ULA-plates versus adherent monolayers [44].

Some HNC cell lines have previously been shown to generate spheroids after 4 days of culture in 96-well ULA-plates [18, 33]. To investigate the use of 384-well ULA-plates to make HNC tumor spheroids for screening, we selected six human HNC cell lines that work in mouse xenograft models and have previously been used for cancer drug discovery [31, 45, 46]. We also selected the HET-1A SV40 T-antigen immortalized human epithelial cell line as a "normal" control, since these cells do not grow as xenograft tumors in immuno-deficient mice [47–50]. We seeded the 6 HNC and HET-1A cell lines at 5,000 cells per well into 384-well ULA-plates and after 24h in culture, Calcein AM (CAM) live and Ethidium homodimer (EHD) dead reagents were added to the wells together with Hoechst stain, and single images per well were acquired with a 4× objective in each of 4 channels on the ImageXpress Micro (IXM) automated high content screen (HCS) platform; transmitted light, Hoechst, FITC and Texas red (Fig. 2A). Each of the 6 HNC tumor cell lines formed 3D spheroids after 24h in ULA-plates, however the sizes of the spheroids and their morphologies, shape and compactness, were different for each tumor cell line (Fig. 2A). In contrast, the HET-1A cells appear to form less compact irregular aggregates after 24h of culture in ULA-plates. The 3D HNC cultures exhibited strong CAM staining in the periphery and throughout the tumor spheroid with only sparse EHD staining in the central core, indicating that the overwhelming majority of the cells in the tumor spheroids are viable (Fig 2A). 3D HNC spheroids produced in ULA-plates can be assayed *in situ* and the tissue culture process can be scaled to provide sufficient throughput for drug screening (Fig. 2). We used Cal33 spheroids produced in 384-well ULA-plates to evaluate the potency and efficacy of three phosphatidylinositol-4,5-bisphosphate 3-kinase (PIK3CA) inhibitors; BEZ-235, BMK-120, and PX-866 (Fig. 2B–D). Cal33 spheroids formed in ULA-plates after 24h in culture were treated with the indicated concentrations of the three PIK3CA inhibitors and returned to the incubator for an additional 72h of culture. Representative transmitted light, Hoechst, CAM and EHD images of Cal33 spheroids exposed to DMSO or selected concentrations of the PIK3CA inhibitors illustrate the effects of these compounds on spheroid size, morphology and viability (Fig. 2B). At the top concentrations of PX-866 and BMK-120 tested, 5 and 50 μM respectively, 72h exposure to these PIK3CA inhibitors dramatically reduced the sizes of the Cal33 spheroids relative to DMSO controls, increased the relative proportion of EHD staining of dead cells, and BMK-120 produced total disintegration of the 3D spheroid structure (Fig. 2B). Although we also observed a significant reduction in the size of the Cal33 spheroids and increased EHD staining relative to DMSO controls with 1.85 μM BEZ-235, a concentration slightly greater than its IC_{50}, treated spheroids remained well defined and contained many viable cells indicated by the strong CAM staining (Fig. 2B). The homogenous Cell Titer Glo™ (Promega, Madison, WI) (CTG) reagent measures the luciferase luminescent signal (RLU's) produced by cellular ATP levels as an indicator of cell number, viability and proliferation and we have previously developed and optimized 384-well 2D HNC growth inhibition assays to determine small molecule cytotoxicity in this format [45, 46]. 3D spheroid growth inhibition assays conducted in ULA-plates have predominantly used the CTG reagent to measure cell viability, cell number and cancer drug effects [18, 33, 43, 44]. To measure the correlation between the RLU signal and number of viable HNC cells in Cal33 spheroids we added the CTG reagent to the wells 24h post seeding at different cell densities into 384-well ULA plates (Fig. 2C). In the 625 to 5,000 cells per well range, the CTG RLU signal increased linearly with the number of Cal33 cells

seeded per well and the sizes of the resulting spheroids (Fig. 2C), but at densities >5K/well the increase in CTG RLU signal was no longer linear. For the HNC spheroid PIK3CA inhibitors growth inhibition assays (Fig. 2D), we used DMSO control wells (Max controls, n=32) to represent uninhibited growth and 200μM Doxorubicin control wells (Min controls, n=32) to represent 100% inhibition of tumor cell growth, and to normalize the data from the compound treated wells as % of DMSO controls (Fig. 2D). The Cal33 spheroid controls exhibited a 6.7-fold assay signal window (S:B ratio) and a Z'-factor coefficient of 0.59, indicating that assay was robust, reproducible and suitable for HTS. The PIK3CA inhibitors inhibited the growth of Cal33 spheroids in a concentration-dependent manner and exhibited IC_{50}s of 1.0, 0.586 and 0.260 μM for BEZ-235, BMK-120, and PX-866 respectively. The production of tumor spheroids in 384-well in ULA-plates occurs *in situ*, does not impose an inordinate tissue culture burden for HTS, is readily compatible with automation and homogeneous assay detection methods, and produces high quality uniform-sized spheroids that can be assayed within days rather than weeks (Table 1).

Polyethylene glycol dimethacrylate (PEGDMA) hydrogel microwell arrays

Heterogeneity in spheroid sizes and shape affect non-cellular factors in the tumor microenvironment including nutrient/oxygen gradients (leading to hypoxia and metabolic stress) that can further impact tumor biology and drug responses. To overcome this challenge, we have micro-fabricated non-adhesive PEGDMA hydrogel microarrays with hundreds of defined diameter microwells (150–600 μm) using photolithography techniques (Fig. 3A) [51]. These non-adhesive microwell arrays enabled generation of uniform, defined size microtumors within 1–2 days using various HNC, breast and cervical cancer cell lines (Fig. 3B, C) [38, 39]. We have recently demonstrated the application of this platform technology to probe activation as well as inhibition of EGFR signaling in 3D HNC microtumors in response to EGF and cetuximab treatments, respectively [38]. Cal33 HNC cells were seeded into 300 μm PEGDMA hydrogel microwells, cultured for 3 days, microtumors were collected, counted and were exposed to 50ng/mL EGF for 15 min. Untreated microtumors were used as controls. Then, the microtumors were fixed in paraformaldehyde, permeabilized with ice cold methanol, and stained with either anti-ERK1/2 or anti-phospho-ERK1/2 antibodies. EGF treatment elevated pERK1/2 levels in Cal33 3D HNC spheroids without affecting total ERK levels. Pre-exposure of Cal33 spheroids to Cetuximab blocked EGF-induced pERK1/2 activation [38].

Another advantage of PEGDMA hydrogel microarrays is their ability to precisely control the microtumor size and thus, the physico-chemical factors in the tumor microenvironment [39]. When noninvasive breast cancer cells (MCF7, T47D) were cultured in non-adhesive PEG hydrogel microwells, precise control over microtumor size enabled controlled changes in tumor microenvironment in a reproducible manner recreating spatial distribution of proliferating and necrotic cells, the development of a hypoxic central core, up-regulation of hypoxia-inducible factor-1 alpha (Hif-1α) and pro-angiogenic vascular endothelial growth factor (vegf) and the overexpression of Glut-1 (metabolic stress marker) in large (600 μm) microtumors of breast cancer cell lines (Fig. 3D,E) [39]. Interestingly, large microtumors of these non-invasive breast cancer cell lines consistently acquired mesenchymal phenotype, migratory phenotype (Fig. 3F), loss of ER-α, and resistance to tamoxifen therapy

recapitulating some of the clinical signatures of tumor progression [39]. By manipulating tumor size (and size alone) and without any other artificial culture conditions, we were able to produce 3D cultures derived from the same noninvasive cells with phenotypic differentiation characteristics representing more advanced stages of tumor progression. Thus, PEGDMA hydrogel microwell arrays provide alternative methods to study the size-induced mechanisms of breast tumor progression *in vitro* using a single cell line model without gene manipulations or switching between cell lines with different phenotypes. They reproducibly generate uniform and defined microtumor sizes, and have the ability to model tumor progression within a short period of 6 days. In addition, unlike 3D spheroid methods that produce one spheroid per well, hydrogel microarrays have the potential to generate multiple spheroids in each well thereby providing intra-well replicates to further enhance the robustness of HTS assays and data analysis. However, several challenges related to automation and handling of these microtumors will need to be overcome before interfacing PEGDMA platform technology with HTS (Table 1).

Conclusions

The physiological relevance and advantages of 3D tumor cell culture models over conventional 2D culture models in cancer biology and drug screening have been widely acknowledged. Although the field is rapidly transitioning to incorporate 3D culture models into early cancer drug screening, the published data only describe applications limited to HTS pilot screens or potency evaluations for small numbers of lead compounds. Despite the numerous differences in architecture, biology and drug responses that have been described between 2D and 3D tumor cell cultures, the jury is still out as to whether 3D models will indeed “bridge the gap” between early lead discovery and improved cancer drug efficacy in pre-clinical animal models and patient tumors. Many new platform technologies to generate 3D cultures are being developed with spheroid cultures being among the most advanced and popular methods. However, there are many technical challenges related to uniformity, handling, maintenance and the automation of these spheroid cultures that have hampered their widespread use in HTS and early stage lead generation. Strong emphasis on interdisciplinary and collaborative science involving cancer biologists, pharmaceutical scientists, tissue engineers and materials science will be instrumental in moving the drug discovery process away from flat 2D biology into the third dimension!

Acknowledgments

SS acknowledges funding support from the NIH (EB018575) and start-up funds from the Department of Pharmaceutical Sciences at University of Pittsburgh. PAJ acknowledges support from a Development Research Project award (Johnston, PI) from the Head and Neck Spore P50 (Ferris and Grandis, CA097190) of the University of Pittsburgh Cancer Institute.

References

1. Al-Lazikani B, Banerji U, Workman P. Combinatorial drug therapy for cancer in the post-genomic era. Nat Biotechnol. 2012; 30:679–92. [PubMed: 22781697]
2. Ocana A, Pandiella A, Siu LL, Tannock IF. Preclinical development of molecular-targeted agents for cancer. Nat Rev Clin Oncol. 2011; 8:200–209.

3. Ocaña A, Pandiella A. Personalized therapies in the cancer “omics” era. Mol Cancer. 2010; 9:202–214. [PubMed: 20670437]
4. Hait W. Anticancer Drug Development: the grand challenges. Nat Rev Drug Discovery. 2010; 9:253–254. [PubMed: 20369394]
5. Hutchinson L, Kirk R. High drug attrition rates–where are we going wrong? Nat Rev Clin Oncol. 2011; 8:189–190. [PubMed: 21448176]
6. Gao HKJ, Ferretti S, Monahan JE, Wang Y, Singh M, Zhang C, Schnell C, Yang G, Zhang Y, Balbin OA, Barbe S, Cai H, Casey F, Chatterjee S, Chiang DY, Chuai S, Cogan SM, Collins SD, Dammassa E, Ebel N, Embry M, Green J, Kauffmann A, Kowal C, Leary RJ, Lehar J, Liang Y, Loo A, Lorenzana E, Robert McDonald E 3rd, McLaughlin ME, Merkin J, Meyer R, Naylor TL, Patawaran M, Reddy A, Röelli C, Ruddy DA, Salangsang F, Santacroce F, Singh AP, Tang Y, Tinetto W, Tobler S, Velazquez R, Venkatesan K, Von Arx F, Wang HQ, Wang Z, Wiesmann M, Wyss D, Xu F, Bitter H, Atadja P, Lees E, Hofmann F, Li E, Keen N, Cozens R, Jensen MR, Pryer NK, Williams JA. Sellers High-throughput screening using patient-derived tumor xenografts to predict clinical trial drug response. Nat Med. 2015; 21:1318–25. [PubMed: 26479923]
7. Hidalgo M, Amant F, Biankin AV, Budinská E, Byrne AT, Caldas C, Clarke RB, de Jong S, Jonkers J, Mælandsmo GM, Roman-Roman S, Seoane J, Trusolino L, Villanueva A. Patient-derived xenograft models: an emerging platform for translational cancer research. Cancer Discov. 2014; 4:998–1013. [PubMed: 25185190]
8. Izumchenko E, Meir J, Bedi A, Wysocki PT, Hoque MO, Sidransky D. Patient-derived xenografts as tools in pharmaceutical development. Clin Pharmacol Ther. 2016; 99:612–621. [PubMed: 26874468]
9. Abbot A. Biology’s new dimension. Nature. 2003; 424:870–872. [PubMed: 12931155]
10. Pampaloni F, Reynaud EG, Stelzer EH. The third dimension bridges the gap between cell culture and live tissue. Nat Rev Mol Cell Biol. 2007; 8:839–45. [PubMed: 17684528]
11. Ryan S, Baird AM, Vaz G, Urquhart AJ, Senge M, Richard DJ, O’Byrne KJ, Davies AM. Drug Discovery Approaches Utilizing Three-Dimensional Cell Culture. Assay Drug Dev Technol. 2016; 14:19–28. [PubMed: 26866750]
12. Zips D, Thames HD, Baumann M. New anticancer agents: in vitro and in vivo evaluation. In Vivo. 2005; 19:1–7. [PubMed: 15796152]
13. Baker B, Chen CS. Deconstructing the third dimension: how 3D culture microenvironments alter cellular cues. J Cell Sci. 2012; 125:3015–3024. [PubMed: 22797912]
14. Friedrich J, Seidel C, Ebner R, Kunz-Schughart LA. Spheroid-based drug screen: considerations and practical approach. Nature Protocols. 2009; 4:309–324. [PubMed: 19214182]
15. Lovitt C, Shelper TB, Avery VM. Miniaturized Three-dimensional Cancer Model for Drug Evaluation. Assay Drug Dev Technol. 2013; 11:435–448. [PubMed: 25310845]
16. Lovitt C, Shelper TB, Avery VM. Advanced cell culture techniques for cancer drug discovery. Biology. 2014; 3:345–367. [PubMed: 24887773]
17. Wang C, Tang Z, Zhao Y, Yao R, Li L, Sun W. Three-dimensional in vitro cancer models: a short review. Biofabrication. 2014; 6
18. Ekert J, Johnson K, Strake B, Pardinas J, Jarantow S, Perkinson R, Colter DC. Three-dimensional lung tumor microenvironment modulates therapeutic compound responsiveness in vitro–implication for drug development. PLoS One. 2014; 9
19. Fischbach C, Chen R, Matsumoto T, Schmelzle T, Brugge JS, Polverini PJ, Mooney DJ. Engineering tumors with 3D scaffolds. Nat Methods. 2007; 4:855–860. [PubMed: 17767164]
20. Härmä V, Virtanen J, Mäkelä R, Happonen A, Mpindi JP, Knuuttila M, Kohonen P, Lötjönen J, Kallioniemi O, Nees M. A comprehensive panel of three-dimensional models for studies of prostate cancer growth, invasion and drug responses. PLoS One. 2010; 5
21. Hongisto V, Jernström S, Fey V, Mpindi JP, Kleivi Sahlberg K, Kallioniemi O, Perälä M. High-throughput 3D screening reveals differences in drug sensitivities between culture models of JIMT1 breast cancer cells. PLoS One. 2013; 8
22. Horman S, To J, Orth AP. An HTS-compatible 3D colony formation assay to identify tumor specific chemotherapeutics. J Biomol Screen. 2013; 18:1298–1308. [PubMed: 23918920]

23. Shin C, Kwak B, Han B, Park K. Development of an in vitro 3D tumor model to study therapeutic efficiency of an anticancer drug. Mol Pharm. 2013; 10:2167–2175. [PubMed: 23461341]
24. Wenzel C, Riefke B, Gründemann S, Krebs A, Christian S, Prinz F, Osterland M, Golfier S Räse S, Ansari N, Esner M, Bickle M, Pampaloni F, Mattheyer C, Stelzer EH, Parczyk K, Prechtl S, Steigemann P. 3D high-content screening for the identification of compounds that target cells in dormant tumor spheroid regions. Exp Cell Res. 2014; 323:131–143. [PubMed: 24480576]
25. Yip D, Cho CH. A multicellular 3D heterospheroid model of liver tumor and stromal cells in collagen gel for anti-cancer drug testing. Biochem Biophys Res Commun. 2013; 433:327–332. [PubMed: 23501105]
26. Alley M, Pacula-Cox CM, Hursey ML, Rubinstein LR, Boyd MR. Morphometric and colorimetric analyses of human tumor cell line growth and drug sensitivity in soft agar culture. Cancer Res. 1991; 51:1247–56. [PubMed: 1705170]
27. Fiebig H, Maier A, Burger AM. Clonogenic assay with established human tumour xenografts: correlation of in vitro to in vivo activity as a basis for anticancer drug discovery. Eur J Cancer. 2004; 40:802–20. [PubMed: 15120036]
28. Thierbach R, Steinberg P. Automated soft agar assay for the high-throughput screening of anticancer compounds. Anal Biochem. 2009; 387:318–20. [PubMed: 19454240]
29. Tveit K, Endresen L, Rugstad HE, Fodstad O, Pihl A. Comparison of two soft-agar methods for assaying chemosensitivity of human tumours in vitro: malignant melanomas. Br J Cancer. 1981; 44:539–44. [PubMed: 7295510]
30. Anderson S, Towne DL, Burns DJ, Warrior U. A high-throughput soft agar assay for identification of anticancer compound. J Biomol Screen. 2007; 12:938–45. [PubMed: 17942786]
31. Lin C, Grandis JR, Carey TE, Gollin SM, Whiteside TL, Koch WM, Ferris RL, Lai SY. Head and neck squamous cell carcinoma cell lines: established models and rationale for selection. Head Neck. 2007; 29:163–188. [PubMed: 17312569]
32. F R. A simple hanging drop cell culture protocol for generation of 3D spheroids. J Vis Exp. 2011; 51
33. Vinci M, Gowan S, Boxall F, Patterson L, Zimmermann M, Court W, Lomas C, Mendiola M, Hardisson D, Eccles SA. Advances in establishment and analysis of three-dimensional tumor spheroid-based functional assays for target validation and drug evaluation. BMC Biol. 2012; 10:29–49. [PubMed: 22439642]
34. Krausz E, de Hoogt R, Gustin E, Cornelissen F, Grand-Perret T, Janssen L, Vloemans N, Wuyts D, Frans S, Axel A, Peeters PJ, Hall B, Cik M. Translation of a tumor microenvironment mimicking 3D tumor growth co-culture assay platform to high-content screening. J Biomol Screen. 2013; 18:54–66. [PubMed: 22923784]
35. Li X, Zhang X, Zhao S, Wang J, Liu G, Du Y. Micro-scaffold array chip for upgrading cell-based high-throughput drug testing to 3D using benchtop equipment. Lab Chip. 2014; 14:471–481. [PubMed: 24287736]
36. Rimann M, Angres B, Patocchi-Tenzer I, Braum S, Graf-Hausner U. Automation of 3D cell culture using chemically defined hydrogels. J Lab Autom. 2014; 19:191–197. [PubMed: 24132162]
37. Tibbitt M, Anseth KS. Hydrogels as extracellular matrix mimics for 3D cell culture. Biotechnol Bioeng. 2009; 103:655–663. [PubMed: 19472329]
38. Singh M, Close DA, Mukundan S, Johnston PA, Sant S. Production of Uniform 3D Microtumors in Hydrogel Microwell Arrays for Measurement of Viability, Morphology, and Signaling Pathway Activation. Assay Drug Dev Technol. 2015
39. Singh M, Mukundan S, Jaramillo M, Oesterreich S, Sant S. Three-Dimensional Breast Cancer Models Mimic Hallmarks of Size-Induced Tumor Progression. Cancer Res. 2016; 76(13):3732–43. [PubMed: 27216179]
40. Haisler W, Timm DM, Gage JA, Tseng H, Killian TC, Souza GR. Three-dimensional cell culturing by magnetic levitation. Nat Protoc. 2013; 8:1940–1949. [PubMed: 24030442]
41. Trask OJ, Moore A, LeCluyse EL. A micropatterned hepatocyte coculture model for assessment of liver toxicity using high-content imaging analysis. Assay Drug Dev Technol. 2014; 12:16–27. [PubMed: 24444127]

42. Zhang Y, Duchamp M, Oklu R, Ellisen LW, Langer R, Khademhosseini A. Bioprinting the Cancer Microenvironment. ACS Biomater Sci Eng. 2016; 2:1710–1721. [PubMed: 28251176]

43. Howes A, Richardson RD, Finlay D, Vuori K. 3-Dimensional culture systems for anti-cancer compound profiling and high-throughput screening reveal increases in EGFR inhibitor-mediated cytotoxicity compared to monolayer culture systems. PLoS One. 2014; 9

44. Rotem A, Janzer A, Izar B, Ji Z, Doench JG, Garraway LA, Struhl K. Alternative to the soft-agar assay that permits high-throughput drug and genetic screens for cellular transformation. Proc Natl Acad Sci U S A. 2015; 112:5708–5713. [PubMed: 25902495]

45. Johnston P, Sen M, Hua Y, Camarco D, Shun TY, Lazo JS, Grandis JR. High-content pSTAT3/1 imaging assays to screen for selective inhibitors of STAT3 pathway activation in head and neck cancer cell lines. Assay Drug Dev Technol. 2014; 12(1):55–79. [PubMed: 24127660]

46. Johnston P, Sen M, Hua Y, Camarco DP, Shun TY, Lazo JS, Wilson GM, Resnick LO, LaPorte MG, Wipf P, Huryn DM, Grandis JR. HCS Campaign to Identify Selective Inhibitors of IL-6-Induced STAT3 Pathway Activation in Head and Neck Cancer Cell Lines. Assay Drug Dev Technol. 2015; 13:356–76. [PubMed: 26317883]

47. Ahrens T, Timme S, Hoeppner J, Ostendorp J, Hembach S, Follo M, Hopt UT, Werner M, Busch H, Boerries M, Lassmann S. Selective inhibition of esophageal cancer cells by combination of HDAC inhibitors and Azacytidine. Epigenetics. 2015; 10:431–445. [PubMed: 25923331]

48. Ahrens T, Timme S, Ostendorp J, Bogatyreva L, Hoeppner J, Hopt UT, Hauschke D, Werner M, Lassmann S. Response of esophageal cancer cells to epigenetic inhibitors is mediated via altered thioredoxin activity. Lab Invest. 2015

49. Fichter C, Gudernatsch V, Przypadlo CM, Follo M, Schmidt G, Werner M, Lassmann S. ErbB targeting inhibitors repress cell migration of esophageal squamous cell carcinoma and adenocarcinoma cells by distinct signaling pathways. J Mol Med (Berl). 2014; 92:1209–1223. [PubMed: 25091467]

50. Stoner G, Kaighn ME, Reddel RR, Resau JH, Bowman D, Naito Z, Matsukura N, You M, Galati AJ, Harris CC. Establishment and characterization of SV40 T-antigen immortalized human esophageal epithelial cells. Cancer Res. 1991; 51:365–371. [PubMed: 1703038]

51. Bae H, et al. Development of functional biomaterials with micro- and nanoscale technologies for tissue engineering and drug delivery applications. Journal of Tissue Engineering and Regenerative Medicine. 2012:1–14.

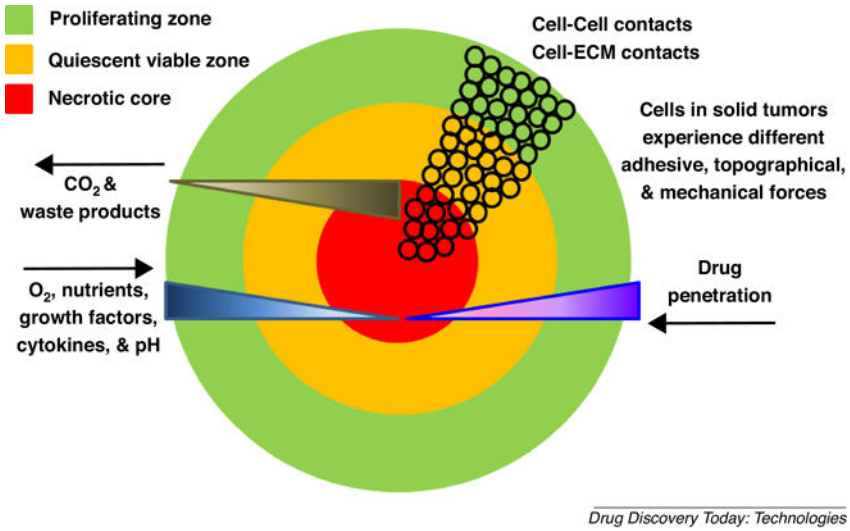

Figure 1. Tumor cells cultured in 3D microenvironments experience different cellular cues that alter their responses and behaviors

Tumor cells cultured in spheroids exist in a highly interactive 3D microenvironment where cell-cell interactions, cell-ECM interactions and local gradients of nutrients, growth factors, secreted factors and oxygen regulate cell function and behavior. Cells in 3D cell cultures are exposed to different adhesive, topographical and mechanical forces than cells growing in 2D on treated surfaces, and the cell-cell and cell-ECM interactions of cells in multi-layer tumor spheroids constitute a permeability barrier through which therapeutic agents must penetrate. The 3D microenvironment alters numerous cellular and functional activities including; morphology, signal transduction, histone acetylation, gene expression, protein expression, drug metabolism, differential zones of proliferation, viability, hypoxia, pH, differentiation (epithelial to mesenchymal transition, EMT), migration, and drug sensitivity.

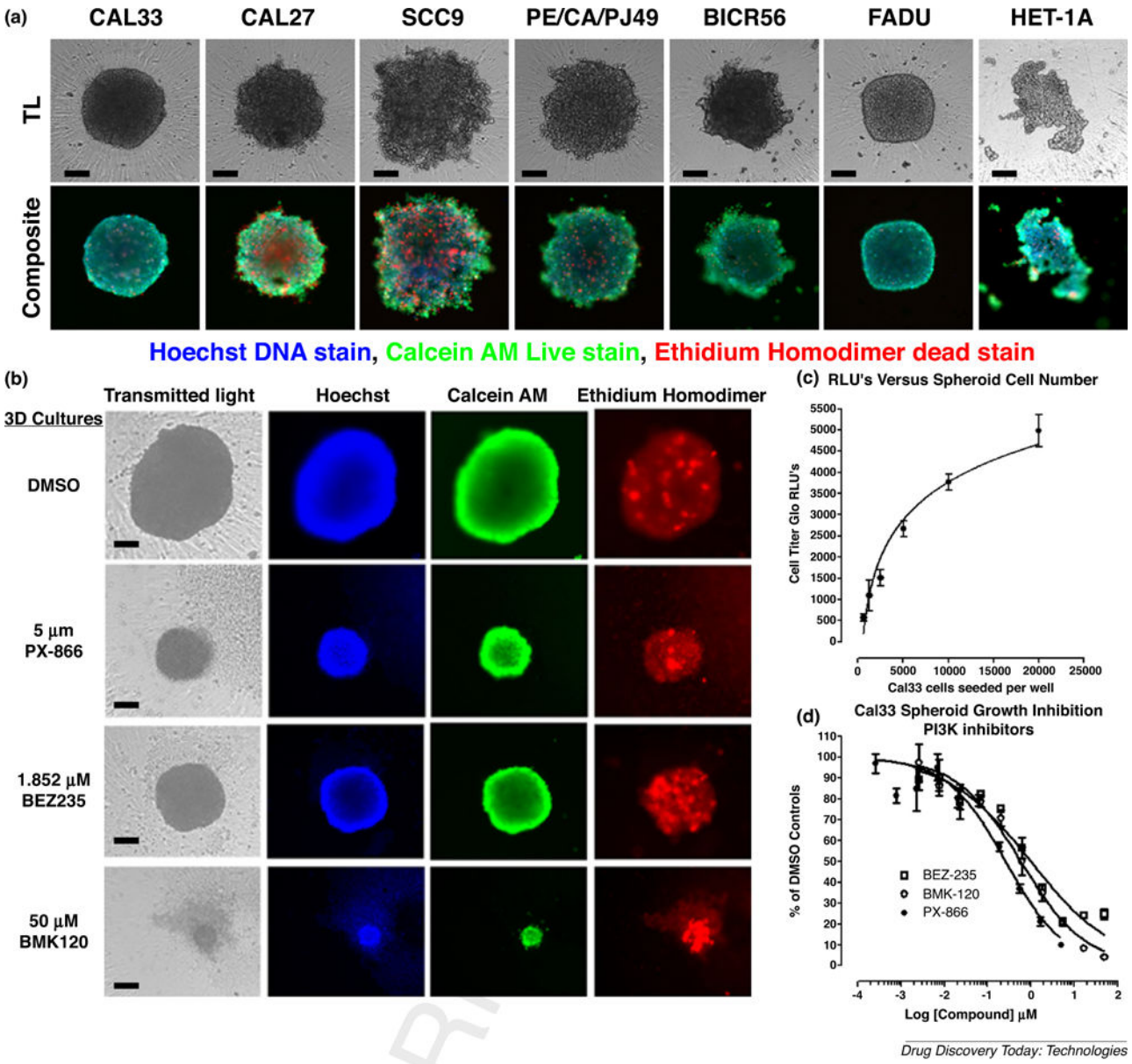

Figure 2. Production and analysis of head and neck cancer spheroids in 384-well ultra-low attachment plates

A. HNC tumor cell lines form Spheroids 24h after seeding in 384-well ULA-plates. We seeded 6 HNC (Cal33, Cal27, PE/CA-PJ-49, SCC9, BICR56 and FADU) and HET-1A cell lines at 5,000 cells per well into 384-well ULA-plates and after 24h in culture Calcein AM (live, green) and Ethidium homodimer (dead, red) reagents were added to the wells at 10 µM, plates were incubated for an additional 45 min before the cells were fixed in para-formaldehyde and stained with Hoechst, and single images per well were acquired with a 4× objective in each of 4 channels on the IXM automated HCS platform (Molecular Devices LLC, Sunnyvale, CA); transmitted light, Hoechst, FITC and Texas red. The scale bar in each of the transmitted light images represents 125 µm (). The diameters of the spheroids formed

by the different HNC cell lines seeded into 384-well ULA-plates ranged between 400 and 600 μm.

B. Transmitted light, Hoechst, CAM and EHD images of Cal33 spheroids exposed to PIK3CA inhibitors for 72h. Cal33 HNC cells were seeded at 5,000 cells per well into 384-well ULA-plates and after 24h in culture the indicated concentrations of the three PIK3CA inhibitors were added to the spheroids and the plates were returned to the incubator for an additional 72h of culture. Calcein AM (live, green) and Ethidium homodimer (dead, red) reagents were added to the wells at 10 μM, plates were incubated for an additional 45 min before the cells were fixed in para-formaldehyde and stained with Hoechst, and single images per well were acquired with a 4× objective in each of 4 channels on the IXM automated HCS platform; transmitted light, Hoechst, FITC and Texas red. The scale bar in each of the transmitted light images represents 125 μm (). The diameters of the Cal33 HNC spheroids exposed to DMSO or the three PIK3CA inhibitors ranged between 125 and 500 μm for 50 μM BMK-120 and DMSO controls respectively.

C. Correlation between Cell Titer Glo® RLU Signal and Cal33 spheroid cell number and size. Cal33 HNC cells were seeded at seeding densities ranging from 625 to 20,000 cells per well into 384-well ULA-plates and after 24h in culture, the Cell Titer Glo™ (Promega, Madison, WI) reagent was added to the wells and the RLU signals were captured on the M5e microtiter plate reader (Molecular Devices LLC, Sunnyvale, CA). The mean ± SD (n=6) RLU signals from six wells for each seeding density are presented. Representative experimental data from multiple independent experiments are shown.

D. Cytotoxicity towards Cal33 spheroids exposed to PIK3CA inhibitors for 72h. Cal33 HNC cells were seeded at 5,000 cells per well into 384-well ULA-plates and after 24h in culture the indicated concentrations of the three PIK3CA inhibitors were added to the spheroids and the plates were returned to the incubator for an additional 72h of culture. After 72h in culture, the CTG reagent was added to the wells and the RLU signals were captured on the M5e microtiter plate reader. For the HNC spheroid growth inhibition assays, we used DMSO control wells (Max controls, n=32) to represent uninhibited growth and 200μM Doxorubicin control wells (Min controls, n=32) to represent 100% inhibition of tumor cell growth respectively, and to normalize the data from the compound treated wells as % of DMSO controls. The mean ± SD (n=3) growth inhibition data from triplicate wells for each compound concentration are presented as the % of the DMSO plate controls. The Cal33 spheroid plate controls exhibited a 6.7-fold assay signal window (S:B ratio) and a Z-factor coefficient of 0.59, indicating that assay was robust, reproducible and suitable for HTS. Representative experimental data from three independent experiments are shown.

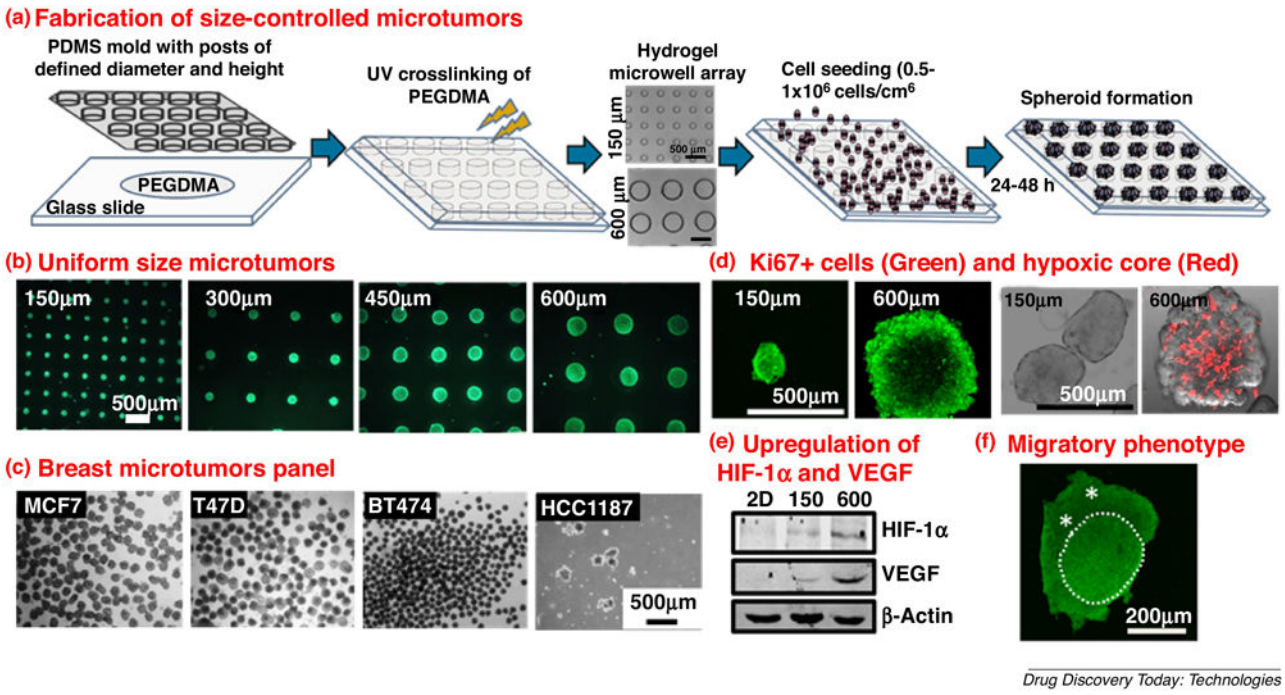

Figure 3. Size-controlled 3D uniform microtumors recapitulate physico-chemical changes in the tumor microenvironment

A. Fabrication of size-controlled microtumors. Schematic showing high throughput production of uniform microtumors on polyethylene glycol dimethacrylate-1000 (PEGDMA) hydrogel microarrays. Defined size (150–600 µm) hydrogel microwell arrays were fabricated using polydimethyl siloxane (PDMS) molds by photo-crosslinking 20% polyethylene glycol dimethacrylate (PEGDMA, 1000Da) solution containing 1% photoinitiator (Irgacure-1959) under OmniCure S2000 UV curing station. Hydrogel devices were seeded with cancer cells ($0.5 – 1.0 \times 10^6/cm^2$) and cultured in 5% CO_2 at 37°C. Non-adhesive PEGDMA microwells facilitated cell-cell adhesion forming uniform microtumors where microwell size controlled the microtumor size.

B. Hydrogel microwell devices containing arrays of uniform size Cal33 microtumors. Microarrays containing microtumors were stained with 2 µM Calcein-AM (live cells) and ethidium homodimer (dead cells) on day 3 and subsequently imaged using fluorescent microscope with 2.5× objective lens.

C. Uniform size microtumors of various breast cancer cell lines. PEGDMA hydrogel microwell arrays (150 µm) were used to fabricate microtumors of subtype-specific breast cancer cell lines. Bright field images showed that hundreds of uniform size microtumors could be fabricated within short duration of 24–48 h. Hormone receptor positive cells (MCF7, T47D and BT474) formed compact microtumors as compared to triple negative breast cancer cell line (HCC1187).

D. Spatial distribution of proliferating cells and hypoxia in 3D. Microtumors were harvested on day 6, fixed and immunostained with proliferation marker Ki-67 overnight followed by staining with respective Alexa flour 488 labeled secondary antibody. Images were obtained on Olympus FluoView confocal microscope using 488nm laser. Large (600 µm) microtumors showed Ki-67 positive proliferating cells only on the periphery unlike

uniformly distributed Ki-67 positive cells in the 150 μm microtumor. Oxygen availability inside the microtumors was determined by staining microtumors harvested on day 6 with oxygen-sensitive fluorescent dye (Ru-dpp, 1×10^{-4} M) for 3 h and imaging under confocal microscope (Olympus Fluoview 1000). Images were captured by confocal microscope using 543-nm He-Ne laser for excitation and 604 LP emission filters. Large microtumors (600 μm) showed enhanced red fluorescence in the center as compared to small microtumors suggesting limited oxygen diffusion in large microtumors.

E. Size-dependent expression of Hif-1α and vascular endothelial growth factor (Vegf) protein. Protein lysates were prepared using day 6 old microtumors along with 2D monolayer cells and western blot was performed using 40–50 μg protein on 8% polyacrylamide gel. Western blot results showed upregulation of Hif-1α and Vegf expression in 600 μm tumors as compared to 150 μm ones.

F. Large microtumors show migratory phenotype. Microtumors were harvested on Day 6, fixed with 4% paraformaldehyde and subsequently with 95% methanol. They were immunostained with anti-E-cadherin primary and respective secondary antibody. Immunostained microtumors (green) were imaged under confocal microscope using 10× objective lens and 488nm laser. Star (*) represents the cells collectively migrated out of the wells from the microtumor.

Table 1

Comparison of *in vitro* 3D Model Strengths and Challenges Related to Cancer Lead Discovery

3D Model Type	Comments	Strengths	Challenges	References
Anchorage-Dependent Models				
Engineered scaffolds: simulate ECM & provide structural &/or physical support	Natural hydrogels of proteins & ECM components. Covalently modified synthetic hydrogels, often based on PEG	Cancer cells encapsulated in micro-porous scaffolds that mimic native ECM & enable cells to adhere, proliferate, spread & migrate in 3D	Natural gel matrices ~ poorly defined myriad of growth factors & endogenous components. Batch to batch variability, & calibration of mechanical & biochemical properties difficult. Gelation temperature shifts hard to automate. Variable Z-plane location of colonies, colony size & shape heterogeneity, & opacity of gel/matrices present challenges for signal capture & analysis. Limit compound or detection reagent penetration. In formats when gels are dispersed & single cells isolated for analysis – loss of spatial information. Utilized to test small numbers of cancer drugs & for pilot screens of ≤1,500 compounds	[13, 15, 19, 20, 22, 23, 34, 36, 37]
Anchorage-Independent Models				
Soft agar colony formation	Gold Standard: anchorage-independent colony formation in semi-solid agar, a defining characteristic of malignantly transformed cells	Clonogenic assays: tumor stem cells from patient tumor samples, PDXs or tumor cell lines. Normal hematopoietic stem cells used to estimate therapeutic index.	Low throughput 2–3 week assays performed in petri dishes, 6-, 12- or 24-well plate formats. 3-layer multi-step assays difficult to automate. Maintaining tumor cell viability in heated agar & preventing agar gelation during liquid transfers. Variable Z-plane locations, heterogeneity in size & shape, & agar opacity make colony counting hard. Labor intensive & experienced assayers required. Utilized to test small numbers of cancer drugs & for pilot screens ≤ 1,500 samples	[12, 22, 26–30]
Spontaneous aggregation, liquid overlay on agarose, hanging drop, spinner flask & rotary cell cultures	Established methods to generate spheroid cultures.	Spontaneous aggregation, spinner flask & rotary cell cultures easy to set up.	Not all tumor cell lines form spheroids. Spheroid transfer to assay plates for spontaneous aggregation, spinner flask & rotary cell cultures. Scalability & generation of irregular 3D cellular aggregates of variable morphologies & sizes. Liquid overlay on agarose & hanging drop assays are complex, labor intensive & protracted. Used to test small numbers of cancer drugs.	[14, 16–17, 21, 24, 25, 32]
Ultra-low attachment plates	U-bottomed plates with hydrophilic, neutrally charged coating. Lack of attachment cues support formation & growth of spheroids or cell aggregates. Spheroid morphology & immuno-staining similar to those grown in agar.	96- & 384-well plates compatible with automation, HCS & homogeneous assays. Tissue culture scalable for HTS, uniform-sized spheroids produced *in situ* within 1–3 days.	Not all tumor cell lines form tight spheroids in ULA-plates, some form cell aggregates. Only a single spheroid produced per well. Utilized to test small numbers of cancer drugs & pilot screens of ≤633 compounds.	[18, 33, 40, 41] Fig. 2.

3D Model Type	Comments	Strengths	Challenges	References
		Used for cancer drug testing, cell migration & invasion assays.		
Inert PEGDMA hydrogels lacking attachment cues	Photolithography micro-fabricated non-adhesive defined-diameter hydrogel arrays of micro-wells produce uniform, size controlled microtumors within 1–2 days	Produces 100s of uniform, defined size micro-tumors within 1–2 days using human cancer cell lines. Compatible with HCS & homogeneous assay detection methods.	Challenges related to automation & handling of microtumors will need to be overcome before the PEGDMA platform technology can be interfaced with HTS.	[38, 39] Fig. 3.